Modeling Hydrogen Separation in High Temperature Silica Membrane Systems

M. C. Duke, J. C. Diniz da Costa, and G. Q. Lu
ARC Centre for Functional Nanomaterials, The University of Queensland, St Lucia, Qld, 4072, Australia

P. G. Gray
Johnson Matthey Fuel Cells, Blount's Court, Sonning Common, Reading RG4 9NH, U.K.

DOI 10.1002/aic.10777
Published online February 1, 2006 in Wiley InterScience (www.interscience.wiley.com).

In this work, a working model is proposed of molecular sieve silica (MSS) multistage membrane systems for CO cleanup at high temperatures (up to 500°C) in a simulated fuel cell fuel processing system. Gases are described as having little interactions with each other relative to the pore walls due to low isosteric heat of adsorption on silica surfaces and high temperatures. The Arrhenius function for activated transport of pure gases was used to predict mixture concentration in the permeate and retentate streams. Simulation predicted CO could be reduced to levels below the required 50 ppmv for polymer electrolyte membrane fuel cell anodes at a stage H_2/CO selectivity of higher than 40 in 4 series membrane units. Experimental validation showed predicting mixture concentrations required only pure gas permeation data. This model has significant application for setting industrial "stretch targets" and as a robust basis for complex membrane model configurations. *AIChE J,* 52: 1729–1735, 2006
Keywords: Mixture modeling, silica membrane, hydrogen separation, CO poisoning, stretch targets

Introduction

For the hydrogen economy to become a reality, it is likely in the next few decades that hydrogen will still be mainly produced from fossil fuels (natural gas or syngas from coal gasification). A major advantage of hydrogen driven fuel cell technology lies in the zero emission promise. However, reformate gas streams for hydrogen production always contain by-products, such as carbon monoxide, which tend to poison the anode catalysts of polymer electrolyte membrane (PEM) fuel cells.[1,2] The removal of CO in the hydrogen stream is a critical yet challenging issue. There have been many developments in reformate cleaning, including membrane technology. Hydrothermally stable molecular sieve silica (MSS) membranes are becoming suitable hydrogen purification candidates for fuel cell and real industrial applications. For example, the DOE in the USA has spent a considerable effort and investment in membrane technology as a candidate for large scale capture of the greenhouse gas, CO_2, from H_2 rich streams. As these applications are likely to contain steam, we have recently developed a new class of hydrothermally stable molecular sieve silica membranes for hydrogen purification.[3]

The governing separation mechanism, molecular sieving, is a fundamentally simple process, whereby smaller molecules, such as H_2, selectively permeate over larger molecules, such as CO_2, CO, and N_2, by size exclusion. There are several models reported in the literature dealing with the molecular transport of gases. When modeling gas transport in micropores, it is understood that surface interaction plays a major role in the diffusion of gases and can be described by Fick's law. Many mixture models have been derived and in many cases include Stefan-Maxwell formalisms,[4-8] irreversible thermodynamics,[9] and fi-

Correspondence concerning this article should be addressed to M. C. Duke at m.duke@uq.edu.au.

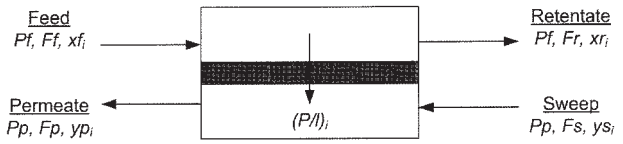

Figure 1. Membrane modeled as a single separation unit.

nite mass exchange.[10-12] The activated transport model originally proposed by Barrer[13] has been extensively used to explain molecular diffusion in MSS membranes. A derivation of Barrer's model to describe molecular sieving permeation in MSS membranes with pores smaller than 4-5Å is in the form[14-24]:

$$\left(\frac{P}{l}\right)_{SA} = \frac{\rho}{l}\frac{1-\varepsilon}{\varepsilon} D_0 K_0 \exp\left(\frac{-E_a}{RT}\right) \tag{1}$$

where $(P/l)_{SA}$ is the permeance (mol.m^{-2}.s^{-1}.Pa^{-1}), r is the density of silica (around 1.8 kg.m^{-3}), and D_0 and K_0 are proportionality constants for activated diffusivity (m^2.s^{-1}) and Henry's law (mol.kg^{-1}.Pa^{-1}), respectively. E_a (kJ.mol^{-1}) is the apparent transport activation energy and is the difference between the mobility energy E_m (kJ.mol^{-1}) and the isosteric heat of adsorption Q_{st} (kJ.mol^{-1}):

$$E_a = E_m - Q_{st} \tag{2}$$

This model describes micropore diffusion to be an activated process governed by an activation energy. In other words, permeation increases with temperature when $E_m > Q_{st}$, contrary to bulk flow and Knudsen diffusion,[16] which always decrease with temperature. In the case of silica microporous membranes, silica has a low adsorption capacity,[20,22,25] mainly complying with Henry's law of low coverage. Hence, Barrer's model could also be used to predict mixture permeation in MSS membranes.

Krishna's extensive works[4,5,26] predicting mixture transport in zeolitic molecular sieve membrane using Stefan-Maxwell has application in the lower temperature region, with highly adsorbing organics. The main feature of inorganic membranes, on the other hand, is their high temperature (>200°C) separation of weakly adsorbing gases, such as H_2, N_2, CO, and CO_2. In fact, the Stefan-Maxwell single file diffusion model reduces to basic single gas Fick-type diffusion when coverage is very low: $\theta_i/\theta_V \approx 0$, where θ_i is the fractional coverage of species i and θ_V is the coverage of vacant sites. Other models to predict mixture transport are mathematically similar to Stefan-Maxwell, such as irreversible thermodynamics, and thus similar simplification would occur. The more recent techniques using non-equilibrium molecular dynamics have been applied on zeolitic and amorphous membranes,[27,28] but development and validation is required before applying the ideal structure permeation to realistic silica membranes.

In this article, we take the Arrhenius function proposed by Barrer for single gases and derive it for a multicomponent system. Based on permeation results for plate membranes and tubes prepared and tested using methods reported elsewhere,[3] multicomponent reformate cleanup is evaluated to verify the performance of the separation system to meet CO 50 ppmv for meeting fuel cell system requirements. The technique is then used to back validate gas permeation results and find suitable "stretch targets" for developing the membrane technology forward.

Membrane Separation Stage Model Development

The membrane separation unit was modeled as a single stage depicted in Figure 1. Known values are feed and permeate pressures, P_f and P_p, respectively, feed flow F_f, feed component i, molar fraction $x_{f,i}$, and sweep flow (if used) F_s, along with the sweep molar fractions of i, $y_{s,i}$.

Unknown values are retentate flow, F_r, retentate molar fraction of i, $x_{r,i}$, permeate flow rate, F_p, and permeate molar fraction of i, $y_{p,i}$. The following assumptions are made in the model:

(1) Henry's law at low pressure and high temperature ensures low surface coverage (surface interactions between gases negligible);

(2) Countercurrent system when sweep gas used;

(3) Sweep gas back-diffusion through membrane is not significant;

(4) Total pressure drop across retentate is negligible;

(5) Total pressure drop across permeate is negligible (though not for hollow fibers[29]);

(6) Mass transfer resistance is confined to the γ-alumina and silica film. The substrate offers insignificant flow resistance;

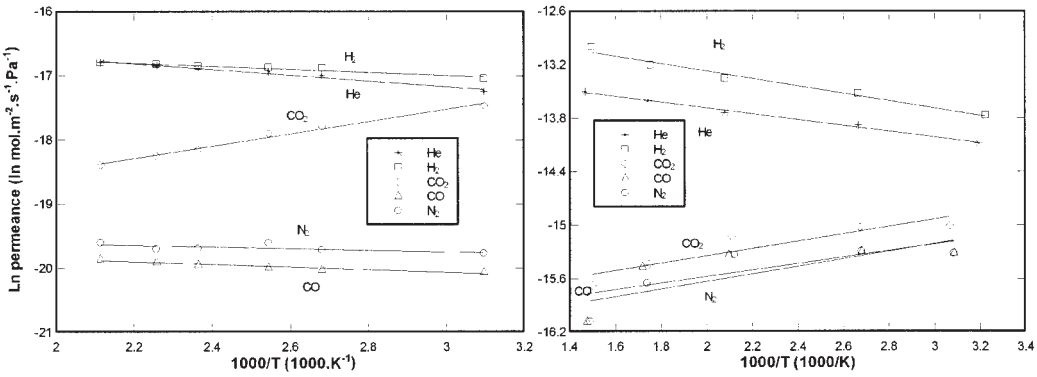

Figure 2. Top layer permeance isosteres for various gases from platelet (left) and tube (right).

Table 1. Apparent Activation Energies, E_a, in kJ · mol^{-1} and r^2 of Eq. 1 Fit for Both Plate and Tube Membranes at 2 Bar Pressure Drop

	He		H_2		CO_2		N_2		CO	
Membrane	E_a	r^2	E_a	r^2	E_a	r^2	E_a	r^2	E_a	r^2
Plate	4.4	0.99	3.6	1.00	−6.9	1.00	9.0	0.99	8.1	0.99
Tube	2.7	0.99	3.5	0.98	−3.4	0.83	−3.5	0.68	−3.0	0.53

(7) There is no mixing of gases in the direction of bulk gas flow;
(8) Plug flow of gases on both sides;
(9) Small scale results are scalable to areas accommodating the required flow rates;
(10) Membrane films are of uniform thickness;
(11) Membrane systems operate at steady state (temperature and pressure);
(12) Partial pressure drop follows a log mean relation; and
(13) Component permeance is constant across the entire membrane surface.

Permeance in the top (selective silica) layers $(P/l)_{TL}$ for each species i was calculated using Eq. 1. Transport through the mesoporous γ-alumina layer is by the non-activated Knudsen diffusion, and assuming Fick's law, Knudsen permeance, $(P/l)_{Kn}$ (mol.m^{-2}.s^{-1}.Pa^{-1}), is given by[30]:

$$\left(\frac{P}{l}\right)_{\gamma} \approx \left(\frac{P}{l}\right)_{Kn} = \frac{d_p \varepsilon}{\tau l}\left(\frac{8}{9\pi MRT}\right)^{1/2} \tag{3}$$

In the case of γ-alumina calcined to 600°C, d_p is 4 nm, ε is 0.55, and τ is 2.2.[31,32] Series analysis of gas diffusion then allows calculation of permeation in each layer from the overall permeance retrieved from experiments $(P/l)_{memb}$ by an analogous circuit resistance equation[33]:

$$\left(\frac{P}{l}\right)^{-1}_{memb} = \left(\frac{P}{l}\right)^{-1}_{substrate} + \left(\frac{P}{l}\right)^{-1}_{\gamma} + \left(\frac{P}{l}\right)^{-1}_{TL} \tag{4}$$

$(P/l)_{memb,i}$ was converted to molar flux exiting in the permeate stream by:

$$F_{p,i} = A\Delta P_{\ln,i}\left(\frac{P}{l}\right)_{memb,i} \tag{5}$$

where A is the membrane permeation area and $\Delta P_{\ln,i}$ is the log mean partial pressure drop of component i:

$$\Delta P_{\ln,i} = \frac{(x_{f,i}P_f - y_{p,i}P_p) - (x_{r,i}P_f - y_{s,i}P_p)}{\ln\left(\frac{(x_{f,i}P_f - y_{p,i}P_p)}{(x_{r,i}P_f - y_{s,i}P_p)}\right)} \tag{6}$$

Since the sweep gas used in the small scale membrane plate was Ar, it does not appear within species i ($y_{s,i} = 0$). The mass balance for each species, i, is:

$$F_f x_{f,i} = F_r x_{r,i} + F_p y_{p,i} \tag{7}$$

Since the retentate consists only of species in set i,

$$\sum x_{r,i} = 1 \tag{8}$$

The flow out of the permeate stream consists of the non-i sweep and all of species i permeating through the membrane:

$$F_p = F_s + F_p \sum x_{p,i} \tag{9}$$

For the condition where no sweep gas was used, $F_s = 0$ and $y_{s,i} = y_{p,i}$ when calculating $\Delta P_{\ln,i}$ at steady state. The four species, H_2, CO_2, N_2, and CO, make the total number of equations using Eqs. 5, 7, 8, and 9 to be 10. This makes a total of 10 unknown parameters that can now be solved by setting the equations to equal zero.

Matlab 6.1 was used to zero find the 10 equations using the "lsqnonlin" optimization package, which solves non-linear equation sets via least squares method. Constraints are permitted with this package to prevent negative number return (ensuring all positive flows). Tolerance was set to give certainty to 1×10^{-6} for all numbers, output as molar fractions (in mol.%) and molar flux (in mol.min^{-1}). Flow rates are input into the model in mol.min^{-1} and pressure is input in bar (absolute). Known values for molar fraction and flow rates were used as initial guesses for unknown values. The initial estimates were calculated first by the arithmetic mean of partial pressure drop instead of Eq. 6. In generating the final answer, Eq. 6 was then used.

Pure Gas Model Parameters

Top layer single gas permeation isosteres from platelets and tube permeation data,[3,34] calculated using the linearized form of Eq. 1, are shown in Figure 2 at a pressure drop of 2 bar. Linear regressions show good fits, as listed in Table 1, indicating membranes of high quality with insignificant contribution of non activated mechanisms. Negative values of E_a for CO_2 were observed on platelets, as supported in the literature.[35] Negative values of E_a were also observed for N_2 and CO on the tube due to its slightly lower selectivity, and hence higher relative value of Q_{st} over E_m (Eq. 2). The differences between the top layer isosteres of the two membranes, although made of the same amorphous silica material, is dependent on a wide range of factors, such as initial substrate surface roughness, top layer gelation conditions, and top layer average thickness. It is this reason that makes modeling from a more fundamental level

Table 2. Pre-Exponential Constant C_0 (×10^{-8} mol · m^{-2} · s^{-1} · Pa^{-1}) from Membrane Permeation Results for Both Plate and Tube Membranes at 2 Bar Pressure Drop

Membrane	He	H_2	CO_2	N_2	CO
Plate	6.92	5.20	0.06	1.21	1.08
Tube	219	396	9.54	6.96	8.69

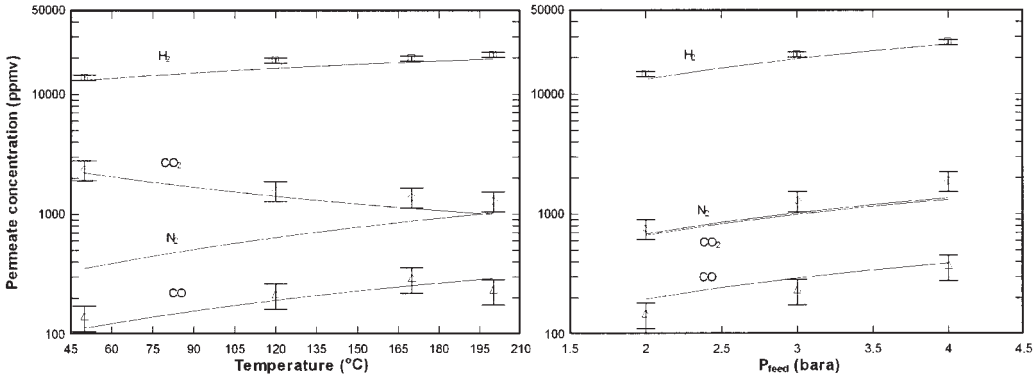

Figure 3. Model results (lines) compared to observed mixture component fraction (symbols) of membrane plate with temperature at 2 bar ΔP (left) and pressure at T = 200°C (right), P_p = 1 bar(abs).

Ar sweep gas used.

difficult, so retrieving single gas permeation from the real membrane compensates for these complexities.

The corresponding fits for the pre-exponential constant are found in Table 2. The lumped constant, C_0 (mol.m^{-2}.s^{-1}.Pa^{-1}) is the combination of the individual constants in Eq. 1:

$$C_0 = \frac{\rho}{l}\frac{1-\varepsilon}{\varepsilon} D_0 K_0 \tag{10}$$

Model Validation

Model results are presented in Figure 3 against observed plate permeate molar fraction from mixture separation experiments with varying temperature and pressure. In these experiments, Ar was used as the sweep gas. Model predictions of H_2, CO_2, and CO were close to experimental values, validating the model under the conditions tested. CO_2 was in all cases slightly higher experimentally, possibly due to its high heat of adsorption, although surface coverage at high temperature is very low in silica derived materials. No experimental data were available to validate the plate N_2 permeate fraction. Tube permeation was similarly validated, including N_2.

Transport Simulation for a Fuel Cell Fuel Processing Unit

Using the model parameters determined from small scale single gas measurements, the activated transport model was extended to predict membrane area and concentration output based on the input gas and flow rate. Molar fractions of dry gases exiting the water-gas shift reactor (WGS) at 1 bar (absolute) in fuel cell systems are listed in Table 3. These values with a total gas flow rate of 15 mol.min^{-1} would give a nominal power output of 10kWe from a fuel cell (FC). Components in this stream are made up mostly of H_2, CO_2, N_2, CO, and CH_4. The kinetic diameters, d_k, of each are 2.89, 3.3, 3.64, and 3.76Å, respectively. The only gas not considered in small and large scale experiments is CH_4 and, since it is slightly larger than CO (d_k, = 3.8 Å) and not considered a problem in fuel cell systems, will be ignored in the following modeling. The requirements of the separation stage are listed in Table 4.

Table 3. Composition of Gas Exiting Water Gas Shift Stage

Gas	WGS (mol %)
H_2	49
CO_2	17
N_2	34
CO	0.5

Single Stage Modeling Results

Simulation results based on the plate model were carried out on a real separation unit, as presented in Table 5. Pressure drop was maintained at 1 bar in simulations. The membrane area, A, is the active membrane surface required to meet the flow rate.

In all cases, a CO reduction in the permeate stream was predicted. When the permeate pressure was 1 bar(abs), CO was only slightly reduced. However, at 0 bar(abs), CO was reduced by a factor of 3 because the permeate was under vacuum. In no case, however, was a single stage able to reduce CO to below the preferred requirement of 50 ppmv (Table 4). The biggest advantage was the predicted increase in H_2 of around 50% in all vacuum permeate cases. The retentate flow was less than the permeate flow and comprised mostly of N_2. A vacuum pump on the permeate side is, therefore, preferable to a compressor on the feed. From further modeling, a vacuum of 10 mbar(abs) or less would be sufficient for this separation. This pressure was chosen to indicate that deep vacuum is not required, justifying the use of a more cost effective pump. A rotary vane vacuum pump to produce 10 mbar(abs) vacuum at the total permeate flow rate would require no more than 800 W power,[36] which is less than 10% of the 10 kW fuel cell output. A less

Table 4. Process Requirements for Membrane Separation Stage in a Fuel Cell CO Cleanup System

Requirement	Value
Pressure drop	1 bar to minimize compression costs
H_2 recovery (ratio of H_2 permeate flow to H_2 feed flow)	At least 95%
CO permeate concentration for FC stack	<50 ppmv (pref.) 100 ppmv (max.)
Operation temperature	390°C (WGS outlet) and 80°C (FC stack inlet)

Table 5. Model Predictions for Real CO Cleanup Operation Using Plate Model Fitting Parameters*

	$T = 390°C$		$T = 80°C$	
Value	$P_p = 0$ Bar(abs)	$P_p = 1$ Bar(abs)	$P_p = 0$ Bar(abs)	$P_p = 1$ Bar(abs)
A	235	624	356	1870
x_{r,H_2}	6.45	25.7	6.79	25.7
x_{r,CO_2}	32.0	26.5	11.12	8.98
x_{r,N_2}	60.7	47.2	80.9	64.6
$x_{r,CO}$	0.865	0.655	1.14	0.785
y_{p,H_2}	74.7	51.3	72.6	51.3
y_{p,CO_2}	7.90	16.0	20.3	17.8
y_{p,N_2}	17.1	32.2	7.01	30.4
$y_{p,CO}$	0.260	0.473	0.123	0.459

*$\Delta P = 1$ bar. Component concentrations in mol · %.

significant vacuum could lead to further parasitic energy reductions, so further using this model, a more in-depth energy optimization is possible.

Using a sweep gas has the same effect as a vacuum in that the partial pressure on the permeate side is reduced, leading to improved efficiency from the same membrane unit. However, sweep gases in real situations can back diffuse through the membrane, which can be significant if the feed pressure is similar to the permeate. This was not the case in our work using argon as the feed pressure and flow conditions were chosen to mitigate back diffusion feed dilution effects. Also, argon molecules are larger than H_2 and CO_2 ($d_k = 3.4$ Å) so back permeation was minor. Sweep gases, which are not easily condensable, are ineffective for industrial scale systems. This is the reason for electing vacuum over sweep gases in our industrially oriented modeling.

Model Extension to Predict Multistage Separation

A string of membrane units, M_k, was modeled to target CO to below the required level. The best separation condition was chosen from Table 5 with vacuum on the permeate side. Best temperature was 390°C for the tube and 80°C for the plate. An example of a 2 stage (M_2) operation is shown in Figure 4.

Table 6 lists the multiple stage modeling results at 1 bar pressure drop with $P_p = 0$ bar(abs) using plate and tube model fitting. An H_2 recovery of 99% was used for each stage to ensure that only after the fifth stage would the total recovery drop below 95%. The higher selectivity plate model predicted that the reduction to below 50 ppmv could be achieved in six stages, with the area totaling to 1452 m^2. After the same number of stages for the tube model, CO was still too high; however, far less area was required to handle the flow as tube permeance was higher, totaling at 19 m^2.

Modeling further stages was not effective as recovery for each stage approached 100%, which significantly reduced the separation efficiency. The partial pressure drop of H_2 over the feed to retentate became steeper with increasing recovery, reducing the average driving force for permeation. On further simulation, it was predicted that an H_2/CO permselectivity of 40 from the tubes would achieve CO reduction below 50 ppmv in only four stages with a total area of only 21 m^2.

This model clearly showed that silica membranes could potentially meet the CO requirements for PEM fuel cell systems. Also, the model was useful in showing which areas of membrane design, such as best selectivity or flux, are needed to set "stretch targets" for technology forecasting. The model could be easily modified for other applications, such as CO_2 capture, to assess these "stretch targets" based on current and/or optimistic individual membrane performance. As mentioned above, H_2/CO separation would be performed very effectively at the target permselectivity of 40 on high flux tubes. It is, therefore, important to achieve at least this selectivity target, made possible with optimized sol-gel methods and coating techniques. Further application of this model could also lead to optimized membrane unit configurations (complex series-parallel systems) where various pressure and/or temperature configurations are used to achieve optimal performance without needing to build prototype systems.

Although fuel processing systems operate close to atmospheric pressure to minimize compression costs, there is possible application in larger scale high pressure WGS systems (around 10 bar) or steam reforming.[37] No data were collected at this high pressure, but pending further study, it is likely that silica membranes could operate at this pressure and modeling could be performed if in the Henry regime. Also, incorporation of steam to the model is necessary for further modeling of real systems. Hydrothermal effects on molecular sieving silica structures have not been clearly defined such that they can be comfortably applied to process modeling, but that is the subject of our current work. With these in mind, successful process modeling of silica membranes will be a key to their success in an effective industrial application in systems such as PEM fuel cells.

Conclusions

From this work, it was shown that pure gas permeance can be used to predict dry MSS membrane permeate output in the Henry's law regime. This can be used as the basis for:

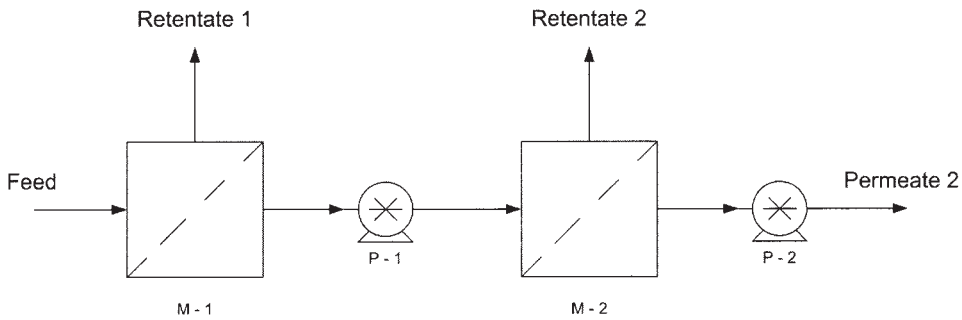

Figure 4. Example 2 stage membrane separation including vacuum pumps after each permeate stream.

Table 6. Multistage Best Membrane Separation Model for Post WGS Using Plate and Tube Model Fitting.*

	Plate Model Stage (T = 80°C)			Tube Model Stage (T = 390°C)		
Value	k = 2	k = 4	k = 6	k = 2	k = 4	k = 6
A (total)	831	1180	1452	10.7	15.8	19.0
x_{r,H_2}	7.28	28.6	40.7	4.03	15.2	34.6
x_{r,CO_2}	17.4	44.1	53.1	32.0	32.4	27.8
x_{r,N_2}	74.1	26.8	6.01	63.1	51.5	36.9
$x_{r,CO}$	1.19	0.561	0.162	0.925	0.851	0.674
y_{p,H_2}	75.0	78.9	80.6	79.9	91.8	96.2
y_{p,CO_2}	21.7	20.6	19.3	7.93	3.65	1.88
y_{p,N_2}	3.20	0.483	0.0871	11.97	4.43	1.91
$y_{p,CO}$	0.0642	0.0127	0.0029	0.202	0.0845	0.0402

*P_f = 1 bar(abs), P_p = 0 bar(abs), overall H_2 recovery = 95%. x_r is retentate and y_r is permeate mol% exiting stage M_k.

- A basic robust module to build complex membrane arrangements with multiple units and pressure/temperature regimes;
- Extension to predict transport with H_2O;
- Setting "stretch targets" that provide membrane flow and selectivity requirements needed for practical process integration; and
- Physical transport understanding to model an MSS membrane reactor system.

Further work will address these conclusions, aimed primarily at optimization of the membrane stage sequence, model extension to predict transport of H_2O, improvements to coating technology leading to CO reductions with less membrane area and energy costs, and further research on MSS membrane reactors. Effective modeling is an essential tool in promoting the potential for MSS membranes in industrial applications, taking advantage of their low cost, high stability, and relatively simple operation.

Acknowledgments

The authors acknowledge support from the Australian Research Council and the Johnson Matthey Fuel Cells Division.

Notation

A = membrane active permeation area (m^2)
C_o = lumped pre-exponential constant for activated transport ($mol.m^{-1}.s^{-1}.Pa^{-1}$)
D_o = pre-exponential diffusivity constant ($m^2.s^{-1}$)
E_a = apparent transport activation energy ($kJ.mol^{-1}$)
E_m = mobility energy ($kJ.mol^{-1}$)
F = flow ($mol.s^{-1}$)
K_o = pre-exponential Henry's constant ($m^2.s^{-1}$)
M = molar mass ($g.mol^{-1}$)
M_k = membrane stage number k
P = total pressure (bar)
ΔP = pressure difference (bar)
PEM = polymer electrolyte membrane
$\left(\frac{P}{l}\right)$or(P/l) = permeance($mol.m^{-2}.s^{-1}.Pa^{-1}$)

Q_{st} = isosteric heat of adsorption ($kJ.mol^{-1}$)
R = ideal gas constant (8.314 $kJ.kmol^{-1}.K^{-1}$)
T = temperature (K unless specified)
d_k = gas molecule kinetic diameter (Å)
d_p = pore diameter (m)
l = membrane thickness (m)
r^2 = linear regression correlation coefficient
x = feed or retentate molar fraction ($mol.mol^{-1}$)
y = permeate or sweep molar fraction ($mol.mol^{-1}$)
ε = porosity (−)
θ = fractional coverage (−)
ρ = density ($kg.m^{-3}$)
τ = tortuosity (−)

Subscripts

Kn = Knudsen
TL = top layer
V = vacant sites
abs = absolute pressure
f = feed
i = gas species *i*
ln = log mean
memb = overall membrane
p = permeate
r = retentate
s = sweep
γ = γ-alumina

Literature Cited

1. Steele BCH, Heinzel A. Materials for fuel-cell technologies. *Nature.* 2001;414:345-352.
2. Korotkikh O, Farrauto R. Selective catalytic oxidation of CO in H_2: fuel cell applications. *Catalysis Today.* 2000;62:249-254.
3. Duke MC, Diniz da Costa JC, (Max) Lu GQ, Petch M, Gray P. Carbonised template molecular sieve silica membranes in fuel processing systems: permeation, hydrostability and regeneration. *J Membr Sci.* 2004;241:325-333.
4. Krishna R, Wesselingh JA. The Maxwell-Stefan approach to mass transfer. *Chem Eng Sci.* 1997;52:861-911.
5. Krishna R. Multicomponent surface diffusion of adsorbed species: a description based on the generalized Maxwell-Stefan equations. *Chem Eng Sci.* 1990;45:1779-1791.
6. Krishna R, Van den Broeke LJP. The Maxwell-Stefan description of mass transport across zeolite membranes. *Chem Eng J and Biochem Eng J.* 1995;57:155-162.
7. Sotirchos SV, Burganos VN. Transport of gases in porous membranes. *MRS Bulletin.* 1999;24:41-45.
8. Van den Broeke LJP, Krishna R. Experimental verification of the Maxwell-Stefan theory for micropore diffusion. *Chem Eng Sci.* 1995; 50:2507-2522.
9. Hwang S-T. Nonequilibrium thermodynamics of membrane transport. 6th World Congress of Chemical Engineering, Melbourne, Australia, 2001.
10. Do DD, Wang K. Dual diffusion and finite mass exchange model for adsorption kinetics in activated carbon. *AIChE J.* 1998;44:68-82.
11. Do DD. A model for surface diffusion of ethane and propane in activated carbon. *Chem Eng Sci.* 1996;51:4145-4158.
12. Wang K, Do DD. Multicomponent adsorption, desorption and displacement kinetics of hydrocarbons on activated carbon—dual diffusion and finite kinetics model. *Separation and Purification Technology.* 1999;17:131-146.
13. Barrer RM. Porous crystal membranes. *J Chem Society, Faraday Transactions.* 1990;86:1123-1130.
14. Uhlhorn RJR, Keizer K, Burggraaf AJ. Gas transport and separation

with ceramic membranes. Part II. Synthesis and separation properties of microporous membranes. *J Membr Sci.* 1992;66:271-287.
15. Shelekhin AB, Dixon AG, Ma YH. Theory of gas diffusion and permeation in inorganic molecular-sieve membranes. *AIChE J.* 1995; 41:58-67.
16. de Lange RSA, Keizer K, Burggraaf AJ. Analysis and theory of gas transport in microporous sol-gel derived ceramic membranes. *J Membr Sci.* 1995;104:81-100.
17. Sea B-K, Watanabe M, Kusakabe K, Morooka S, Kim S-S. Formation of hydrogen permselective silica membrane for elevated temperature hydrogen recovery from a mixture containing steam. *Gas Separation & Purification.* 1996;10:187-195.
18. Bakker WJW, Broeke LJP, Kapteijn F, Moulijn JA. Temperature dependence of one-component permeation through a silicalite-1 membrane. *AIChE J.* 1997;43:2203-2214.
19. Nair BN, Yamaguchi T, Okubo T, Suematsu H, Keizer K, Nakao S-I. Sol-gel synthesis of molecular sieving silica membranes. *J Membr Sci.* 1997;135:237-243.
20. de Vos RM, Verweij H. Improved performance of silica membranes for gas separation. *J Membr Sci.* 1998;143:37-51.
21. Tsai C-Y, Tam S-Y, Lu Y, Brinker CJ. Dual-layer asymmetric microporous silica membranes. *J Membr Sci.* 2000;169:255-268.
22. Diniz da Costa JC, Lu GQ, Rudolph V, Lin YS. Novel molecular sieve silica (MSS) membranes: characterisation and permeation of single-step and two-step sol-gel membranes. *J Membr Sci.* 2002;198:9-21.
23. Hasegawa Y, Ueda A, Kusakabe K, Morooka S. Oxidation of CO in hydrogen-rich gas using a novel membrane combined with a microporous SiO_2 layer and a metal-loaded gamma-Al_2O_3 layer. *Applied Catalysis A: General.* 2002;225:109-115.
24. Lee D, Oyama ST. Gas permeation characteristics of a hydrogen selective supported silica membrane. *J Membr Sci.* 2002;210:291-306.
25. de Lange RSA, Hekkink JHA, Keizer K, Burggraaf AJ, Ma YH. Sorption studies of microporous sol-gel modified ceramic membranes. *J Porous Materials.* 1995;2:141-149.
26. Krishna R, Van den Broeke LJP. The Maxwell-Stefan description of mass transport across zeolite membranes. *Chem Eng J and Biochem Eng J.* 1995;57:155-162.
27. Kobayashi Y, Takami S, Kubo M, Miyamoto A. Non-equilibrium molecular simulation studies on gas separation by microporous membranes using dual ensemble molecular simulation techniques. *Fluid Phase Equilibria.* 2002;194-197:319-326.
28. Pohl PI, Heffelfinger GS. Massively parallel molecular dynamics simulation of gas permeation across porous silica membranes. *J Membr Sci.* 1999;155:1-7.
29. Coker DT, Freeman BD, Fleming GK. Modeling multicomponent gas separation using hollow-fiber membrane contactors. *AIChE J.* 1998; 44:1289-1302.
30. Uhlhorn RJR, Burggraaf AJ. Gas separations with inorganic membranes. In: Bhave RR. *Inorganic Membranes: Synthesis, Characteristics, and Applications*. New York, NY: Van Nostrand Reinhold; 1991: 155.
31. Leenaars AFM, Burggraaf AJ. The preparation and characterization of alumina membranes with ultrafine pores—2. The formation of supported membranes. *J Colloid Interface Sci.* 1984;105:27-40.
32. Uhlhorn RJR, Huis in't Veld MHBJ, Keizer K, Burggraaf AJ. Synthesis of ceramic membranes. *J Membr Sci.* 1992;27:527-537.
33. Meixner DL, Dyer PN. Characterization of the transport properties of microporous inorganic membranes. *J Membr Sci.* 1998;140:81-95.
34. Duke MC, Diniz da Costa JC, Lu GQ, Gray P, Thompsett D. Hydrostability and scaling up molecular sieve silica (MSS) membranes for H_2/CO separation in fuel cell systems. Eighth International Conference on Inorganic Membranes, Cincinnati, OH, 2004;85–88.
35. de Vos RM, Verweij H. High-selectivity, high-flux silica membranes for gas separation. *Science.* 1998;279:1710-1711.
36. Schoonover. Schoonover Technical Downloads—Schoonover Inc., Acworth, GA. URL: http://www.schoonoverinc.com.
37. Tsuru T, Tsuge T, Kubota S, Yoshida K, Yoshioka T, Asaeda M. Catalytic membrane reaction for methane steam reforming using porous silica membranes. *Separation Sci Technology.* 2001;36:3721-3736.

Manuscript received Jun. 23, 2005, and revision received Dec. 21, 2005.